Wireless Channel Simulator Testbed for Airborne Receivers

Steve Blandino[†]
EURECOM
Campus SophiaTech
06410 Biot, France
Email: steve.blandino@eurecom.fr

Florian Kaltenberger
EURECOM
Campus SophiaTech
06410 Biot, France
Email: florian.kaltenberger@eurecom.fr

Michael Feilen
IABG mbH
Einsteinstraße 20
85521 Ottobrunn
Email: feilen@iabg.de

Abstract— **In this paper we introduce an air-to-ground channel model extension for a multi-antenna system. The performance of an aeronautical communication system is strongly influenced by the presence of scatterers and by the three-dimensional (3-D) configuration of transmitter and receiver such as location and velocity. Combined statistical and geometrical models were used to offer a time-space description of the channel. Results of two scenarios are presented: an en-route channel and a takeoff/arrival channel. The implemented frequency selective channel simulator allowed to measure the performances in terms of Bit Error Rate (BER) of an aeronautical system when a single carrier modem, using a $\pi/4$-DQPSK modulation, has been employed. We show that the spreading of the signal in both time and spatial domain sets a BER floor which is strongly dependent on the scenario analyzed and on the power of the Line-of-Sight path. We further extend the model to a multi antenna system an apply different transmission schemes requiring different channel information at the transmitter side. We observe that the complete knowledge of the channel at the transmitter side and knowledge of the direction of the receiver relative to the transmitter yields in similar performance.**

Keywords—3-D channel model, Aeronautical channel modelling, MIMO, beamforming.

I. INTRODUCTION

An Unmanned Aerial Vehicle (UAV) is an aircraft that flies without a human onboard. The crew is totally replaced by a computer system that is pre-programmed before the mission starts or distantly controlled by a human. The need to establish high performance link requires the characterization of the radio communication channel between the UAV and the ground station. In this context, we study an adequate channel model, for a multi-antenna system, able to capture the channel properties between an aircraft and a ground station and we develop a testbed for assessing the baseband modem performance in different scenarios.

In the air-to-ground channels, the aircraft, possibly the ground station and the scattering objects are in motion causing the time variance of the channel. Moreover, due to the long distance between transmitter and receiver the multipath components are often resolvable at the receiver making the channel frequency selective. The increasing demand for performance in terms of data rate, error rate and spectral efficiency, has consolidated the introduction of Multiple Input Multiple Output (MIMO) technology in several communication systems. [1]

has shown that in air-to-ground communication, the effect of multipath interference and shadowing (caused by changes of orientation when the UAV is maneuvering) can be alleviated by the use of directive antennas on the ground and multiple antennas on the UAV, providing a more robust radio channel. The performance of the MIMO system is strongly conditioned on the radio propagation channel. Therefore, accurate modeling of MIMO channels, taking into account the directional properties of the channel, is necessary.

One of the earlier reference that focus on air-ground study is [2], in which the aeronautical mobile radio channel is analyzed and a stochastic narrowband model is proposed. Considering the environment and the different aircraft states during the flight, [3] attempts a complete description of the channel and proposes a wideband channel model featuring parking and taxi environments, takeoff and landing situations, and en-route scenarios for ground-air and air-air links. On the other hand, Geometry-Based Stochastic Channel Models (GSCMs) have gained much attention in MIMO channel modeling due to their capability of modeling spatial and temporal correlation properties in a straightforward manner and the capability to give an easy way to provide the angular impulse response. In [4], for example, a geometric channel model for simulation and analysis of air-to-ground communication is presented. Specifically, with an assumed single-bounce scattering condition, joint probability density function for delay and angle of arrival are derived as a function of the elevation angle.

In this paper we present a novel air-to-ground channel model for multi-antenna systems. The model is based on the scenarios presented in [3]. The extension of the scenarios to a multi-antenna system is based on the angular description proposed in [4].

The paper is structured as follows: Section II describes the aeronautical physical channel model which is extended for a multi-antenna system. Section III describes the structure of the system. Section IV proposes examples of performance evaluation in different scenario. Finally Section V gives the conclusion.

II. AIRBORNE CHANNEL MODEL

A. Double Directional impulse response

The channel is modeled by using a tapped delay line model. The temporal and angular dispersion effects of the

---

time-, delay- variant channel can be described by the Double-Directional Impulse Response (DDIR) [5]:

$$h(t,\tau,\mathbf{\Omega}^{\text{Tx}},\mathbf{\Omega}^{\text{Rx}}) = \tilde{a}_{\text{LOS}}(t)\delta(t-\tau_1)\delta(\mathbf{\Omega}-\mathbf{\Omega}_1^{\text{Tx}})\delta(\mathbf{\Omega}-\mathbf{\Omega}_1^{\text{Rx}})+$$

$$\sum_{k=2}^{L}\tilde{a}_k(t)\delta(\tau-\tau_k)\delta(\mathbf{\Omega}-\mathbf{\Omega}_k^{\text{Tx}})\delta(\mathbf{\Omega}-\mathbf{\Omega}_k^{\text{Rx}})$$

$$(1)$$

where L is the number of taps, the term $\tilde{a}_k(t)$ refers to the complex coefficient of the kth tap and τ_k is the delay of the kth tap. $\tilde{a}_{\text{LOS}}$ is the complex channel gain for the Line-of-Sight (LOS) arriving with the propagation delay $\tau = \tau_1$ and it is modeled as a deterministic process depending on the path loss. Each of the taps for $k = 2, \ldots, L$ represents a delayed NLOS signal and it is expressed as the superposition of N unresolvable path:

$$\tilde{a}_k(t) = \frac{1}{\sqrt{N}}\sum_{i=1}^{N}e^{j\theta_i}e^{2\pi f_{D_i}t} \tag{2}$$

where the factor $\dfrac{1}{\sqrt{N}}$ ensures unitary total power, θ_i is a random angle in $[-\pi,\pi)$ and f_{D_i} is the Doppler shift in $[-f_{D_{\min}}, f_{D_{\max}}]$.

The power of the LOS has been set to:

$$\mathbb{E}[|\tilde{a}_{\text{LOS}}|^2] = P_{\text{LOS}} = \frac{K}{K+1} \tag{3}$$

while the power of the diffuse component is:

$$\mathbb{E}\left[\sum_{k=2}^{L}|\tilde{a}_k|^2\right] = P_{\text{NLOS}} = 1 - P_{\text{LOS}} = \frac{1}{K+1} \tag{4}$$

where K, the so-called Rice factor, represents the ratio between the power of LOS path and that of the diffuse multipath components.

The angular dispersion is described in terms of azimuth and elevation assuming $\mathbf{\Omega}^{\text{Tx}} = (\phi, \rho)$ and $\mathbf{\Omega}^{\text{Rx}} = (\psi, \nu)$ where ϕ and ψ are the Direction of Departure (DoD) and Direction of Arrival (DoA) azimuth angles respectively and ρ and ν are the DoD and DoA elevation angles respectively.

The double directional impulse response describes only the pure propagation channel. It does not include any information about the system such as type of antenna, antenna configuration, system bandwidth or pulse shaping.

B. Channel Scenario

The different conditions of an aircraft during flight lead to different channel scenarios [3]. If the aircraft is an airborne object, two channel models can be identified: the en-route channel and the arrival/takeoff channel.

1) En-route Channel Model: the en-route scenario can be applied when the aircraft is airborne far from the ground station. The propagation path between aircraft and ground terminals is characterized not only by a direct LOS path, but also by multipath reflections. The en-route scenario, as shown in [6], can be described by using a two rays model:

- An LOS component arriving with the propagation delay;

- A cluster of reflected and delayed paths due to the scatterer objects (on the Earth's surface).

The direct path can be modeled as a deterministic function depending on the path loss while the diffuse component can be modeled as a Rayleigh process. The delay probability density function (pdf) can be written as:

$$p(\tau) = \frac{K}{K+1}\delta(\tau-\tau_1) + \frac{1}{K+1}\delta(\tau-\tau_{\max}) \tag{5}$$

from which the Power Delay Profile (PDP) in Figure 1 can computed making the WSSUS assumption and following the proof in [7].
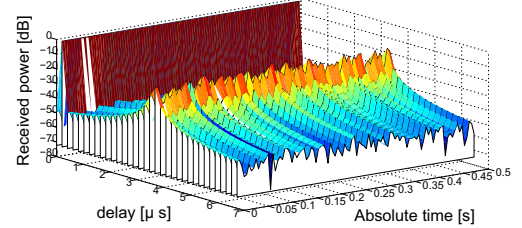

Fig. 1: Time varying time-delay profile for en-route scenario.

2) Arrival/Takeoff Channel Model: the arrival/takeoff scenario is applied when the aircraft is still airborne but has already left its cruising speed and altitude, and is about to land, and vice versa. The PDP is likely to switch from a two-ray scenario towards a rural area characteristic. The delays are in this case well described by an exponential decay as in Figure 2 and the pdf of such a one-sided delay power spectrum is expressed by:

$$p(\tau) = \begin{cases} \dfrac{1}{\tau_{\text{slope}}(1-e^{-\tau_{\max}/\tau_{\text{slope}}})}e^{-\tau/\tau_{\text{slope}}} & \text{if } 0 < \tau \leq \tau_{max} \\ 0 & \text{else} \end{cases}$$
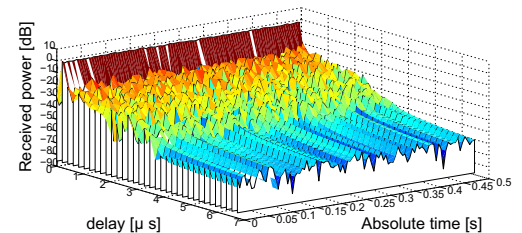
$$(6)$$

Fig. 2: Time varying time-delay profile for arrival/takeoff scenario.

C. Angular description

To obtain the double directional model in equation (1), the description of the DoA and DoD can be provided by using GSCMs model [8]. The basic idea behind the GSCMs is to simulate the radio channel introducing randomly scattering objects modifying the environment and obtaining a simulation environment closer to the real propagation channel. In particular a Geometrically-Based Single Bounce Elliptical Model (GBSBEM) has been used to generate the position of the
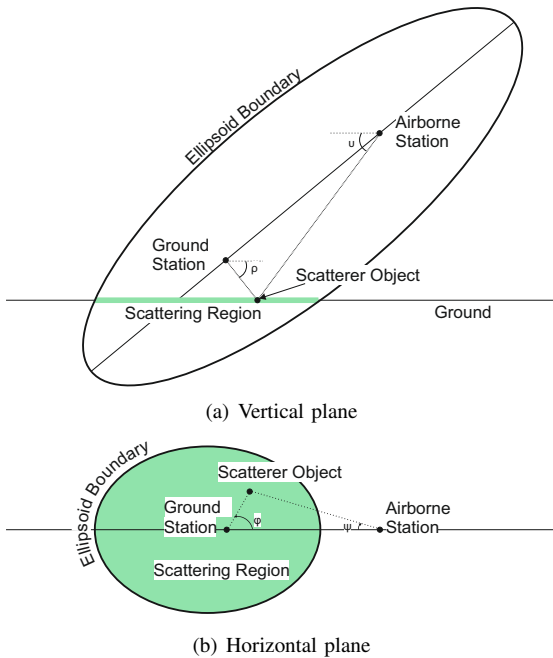
(a) Vertical plane

(b) Horizontal plane

Fig. 3: Geometry of the of the air-to-ground scenario

Fig. 4: Tapped delay line model for MIMO matrix

channel h_{11}:

$$h_{nm} = \int_{\mathbf{\Omega}^{\text{Tx}}} \int_{\mathbf{\Omega}^{\text{Rx}}} G_m^{\text{Tx}}(\mathbf{\Omega}^{\text{Tx}}) h_{11}(t, \tau, \mathbf{\Omega}^{\text{Tx}}, \mathbf{\Omega}^{\text{Rx}}) \cdot$$
$$\cdot \, G_n^{\text{Rx}}(\mathbf{\Omega}^{\text{Rx}}) \mathrm{e}^{-j\mathbf{k}\cdot m\mathbf{d}^{\text{Tx}}} \mathrm{e}^{-j\mathbf{k}\cdot n\mathbf{d}^{\text{Rx}}} d\mathbf{\Omega}^{\text{Tx}} \, d\mathbf{\Omega}^{\text{Rx}} \quad (7)$$

where the terms $G_m^{\text{Tx}}(\mathbf{\Omega}^{\text{Tx}})$ and $G_n^{\text{Rx}}(\mathbf{\Omega}^{\text{Rx}})$ denote the element radiation pattern, including the mutual coupling effect, $\mathbf{d}^{\text{Tx}}$ and $\mathbf{d}^{\text{Rx}}$ indicate respectively the distances between the antenna elements at the transmitter and at the receiver and $\mathbf{k}$ denotes the wave vector.

The final representation of the MIMO channel matrix is still a tapped delay line model as in Figure 4. Each of the tap is represented by a matrix and again the first tap represents the LOS path.

III. SYSTEM DESCRIPTION

The proposed channel model was then applied to a single carrier modem. The transmitter consists of a random binary data generator that delivers to the modulator a bit stream, which is modeled as independent identically distributed random variables. The information bit stream is then mapped into a $\frac{\pi}{4}$-DQPSK constellation.

A MIMO $N_{\text{Tx}} \times N_{\text{Rx}}$ is considered. The downlink transmitter sends $N_s \leq N_{\text{Tx}}$ parallel data streams which are mapped to the N_{Tx} antenna element of the transmitter array through the $N_{\text{Tx}} \times N_s$ precoder matrix $\mathbf{V}[k, \tau]$. The transmitted channel symbol vector in a symbol period is therefore:

$$\mathbf{x} = \mathbf{V}\tilde{\mathbf{x}} \quad (8)$$

where $\tilde{\mathbf{x}}$ is the N_s-dimensional data symbol vector such that $\mathbb{E}[|\tilde{x}|^2] = \sigma_s^2$. The input-output relation in a time-delay variant MIMO system can expressed as

$$\mathbf{y}[k] = \frac{1}{\sqrt{N_{\text{Tx}}}} \sum_{\tau_i=1}^{L} \mathbf{H}[k, \tau_i] \mathbf{x}[k - \tau_i] + \mathbf{n}[k] \quad (9)$$

where $\mathbf{y}$ is the received N_{Rx}-dimensional channel symbol vector, $\mathbf{H}$ is the L-taps $N_{\text{Rx}} \times N_{\text{Tx}}$ MIMO matrix, $\mathbf{n} \sim \mathcal{NC}(0, \sigma_n I)$ is the N_{Rx}-dimensional additive white Gaussian noise vector and $\frac{1}{\sqrt{N_{\text{Tx}}}}$ is used to ensure $\mathbb{E}[|\tilde{\mathbf{x}}|^2] = \sigma_s^2$.

The transmitted symbols totally overlap in both time and frequency. As a consequence, inter-stream interference degrades the received signals. The receiver must separate the data symbols and retrieve the data by means of detection. Using the $N_s \times N_{\text{Rx}}$ detector filter $\mathbf{U}[k, \tau]$, the received data symbol vector is:

$$\tilde{\mathbf{y}}[k] = \frac{1}{\sqrt{N_{\text{Tx}}}} \sum_{\tau_i=1}^{L} \mathbf{U}[k, \tau]^H \mathbf{H}[k, \tau_i] \mathbf{x}[k - \tau_i] + \tilde{\mathbf{n}}[k]. \quad (10)$$

scatterers and then to compute the angular description [4]. The air to ground channel model implemented is based on a three-dimensional ellipsoidal geometry, that has ground station and aircraft as a focal points. Figures 3(a) and 3(b) describe the ellipsoidal geometry respectively in the vertical and horizontal plane. In this model all the scatterers can lie inside the ellipsoid boundary determined by the multipath component with maximum delay. Assuming the scatterers located on the ground as in [4], the scattering region is the intersection between the ellipsoid and the horizontal plane as shown in Figure 3(a).

The spatial properties of the channel have been correlated with the temporal description already given in (5) and (6). The different delays determine different scattering subregions on which scatterers have been uniformly generated with the acceptance-rejection method [9]. Finally, using the scatterer positions, DoA and DoD has been easily computed, in both azimuth and elevation.

D. From DDIR to MIMO matrix

The MIMO channel matrix describes the channel on a system level including the antenna properties. The MIMO channel matrix should be retrieved from the description of the all combinations h_{nm} in which $n = 1, \ldots, N_{\text{Rx}}$ represents the receiving antenna element and $m = 1, \ldots, N_{\text{Tx}}$ represents the transmit antenna element, where N_{Rx} and N_{Tx} denote respectively the number of receiver and transmitter antenna elements. Under three assumption (the narrowband and balanced array assumption as well as the plane wave assumption [10]) it is possible to write the matrix having the knowledge of a single
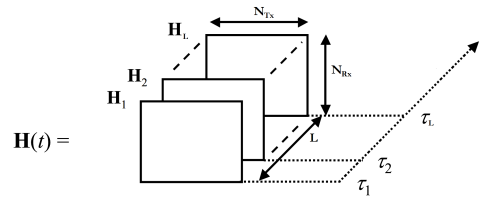
Different transmission schemes can be applied to recover the right transmitted data symbols, depending on the channel state information available at the transmitter side.

A. Partial Channel State Information

Let's assume the transmitter knows the position of the receiver but has no knowledge about the channel. The transmission of the discrete valued data symbols must be implemented via the transmit antenna without precoding. A possible strategy for the transmitter is to change the direction of the beam by changing the coefficient $G_j^{\text{Tx}}(\mathbf{\Omega}^{\text{Tx}})$. The N_s data streams sent on the transmit antennas all arrive cross-coupled at the receiver. The receiver can separate the data streams exploiting the knowledge of the channel matrix $\mathbf{H}$, e.g. using a linear Zero Forcing or MMSE filter. In practice, the elements of $\mathbf{H}$ are estimated by using probe signals.

B. Perfect Channel State Information

When the channel is fully known at the transmitter, digital beamforming can be exploited jointly designing an adequate pre-coder $\mathbf{V}[k,\tau]$ at the transmitter side and an opportune decoder $\mathbf{U}[k,\tau]$ at the receiver side. From basic linear algebra the matrix $\mathbf{H}$ has a singular value decomposition (SVD):

$$\mathbf{H}[k,\tau] = \hat{\mathbf{U}}[k,\tau]\mathbf{\Sigma}[k,\tau]\hat{\mathbf{V}}^H[k,\tau] \qquad (11)$$

where:

- $\hat{\mathbf{U}}[k,\tau]$ is an $N_{\text{Rx}} \times N_{\text{Rx}}$ matrix such that $\hat{\mathbf{U}}^H[k,\tau]\hat{\mathbf{U}}[k,\tau] = \mathbf{I}$.

- $\hat{\mathbf{V}}[k,\tau]$ is an $N_{\text{Tx}} \times N_{\text{Tx}}$ matrix such that $\hat{\mathbf{V}}^H[k,\tau]\hat{\mathbf{V}}[k,\tau] = \mathbf{I}$.

- $\mathbf{\Sigma}[k,\tau]$ is a diagonal matrix with nonnegative singular values σ_r, $r = 1,\ldots,\min(N_{\text{Tx}},N_{\text{Rx}})$.

Designing $\mathbf{U}[k,\tau] = \hat{\mathbf{U}}[k,\tau]$ and $\mathbf{V}[k,\tau] = \hat{\mathbf{V}}[k,\tau]$ the received data symbols are:

$$\tilde{\mathbf{y}}[k] = \frac{1}{\sqrt{N_{\text{Tx}}}}\sum_{\tau_i=1}^{L}\mathbf{\Sigma}[k,\tau_i]\tilde{\mathbf{x}}[k-\tau_i] + \tilde{\mathbf{n}}[k]. \qquad (12)$$

The (12) is the equivalent system of the original (9) and it can be seen as a set of parallel input-output relation. Each output $r, r = 1,\ldots,\min(N_{\text{Tx}},N_{\text{Rx}})$ of the equivalent system can be written as:

$$\tilde{y}_r[k] = \frac{1}{\sqrt{N_{\text{Tx}}}}\sum_{\tau=1}^{L}\sigma_r[k,\tau]\tilde{x}_r[k-\tau] + \tilde{n}_r[k] \qquad (13)$$

and the term σ_r is usually referred as *eigen-channel*.

IV. PERFORMANCE EVALUATION

A. Analysis of the MIMO channel matrix properties

The $\mathbf{H}$ matrix has different behavior depending on the environment condition. The rank of $\mathbf{H}$ and the gain of the eigen-channel with better condition σ_1 give a measure of the channel condition in strong LOS application.

The follow example refers to the arrival scenario and the $\mathbf{H}$ matrix is normalized such that $\mathbb{E}[|\mathbf{H}|^2] = N_{\text{Tx}} \cdot N_{\text{Rx}}$.
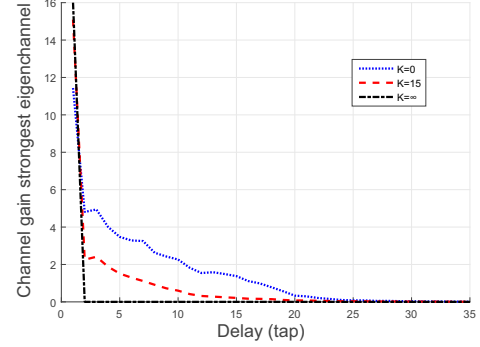

Fig. 5: σ_1 varying the delay. Decreasing the K factor the energy of the channel spreads over the taps.
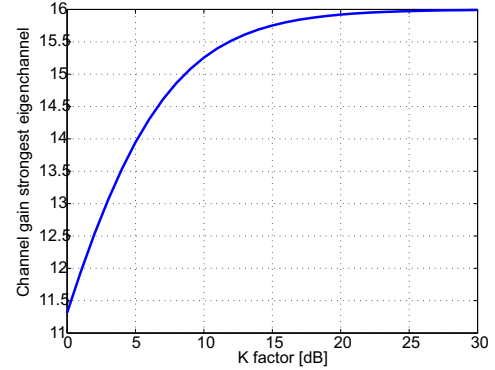

Fig. 6: σ_1 varying the K factor.

The channel properties are evaluated over a 16×16 MIMO system. Both transmitter and receiver have the use of 4×4 rectangular array operating at 5 GHz and spaced by $\frac{\lambda}{2}$ in both dimensions. Each antenna elements has an omni-directional antenna pattern.

Figure 5 shows the behavior of $\sigma_1[\tau]$ for different K factors. The smaller the K factor, the wider the delay spread. For $K \to \infty$ the channel tends to become non dispersive, i.e. AWGN. The gain of the channel is maximum for the LOS tap. Focusing the analysis on the LOS tap, Figure 6 shows $\sigma_1[K]$ fixing $\tau = \tau_1$. After $K \geq 25\,\text{dB}$ it becomes the only path present. Figure 7 shows the variation of the rank of $\mathbf{H}$ with the delay for different distances, fixing $K = 15$ dB. In both cases, $d = 700\,\text{m}$ and $d = 2000\,\text{m}$, because of the strong LOS component, the first tap does not have dispersion in the angular domain. As a result the $\mathbf{H}$ matrix is rank deficient. The successive taps are affected by the influence of the scatterers present in the ground and the channel spreads in the angular domain, so the rank of the matrix increases. The closer the aircraft, the higher the effects of the scatterers, that means that, a higher rank is obtained for lower distances.

B. System Implementation

Our system model from Section III assumes that the channel has memory and thus models a frequency selective channel. The actual design of the transmitter and the receiver however is
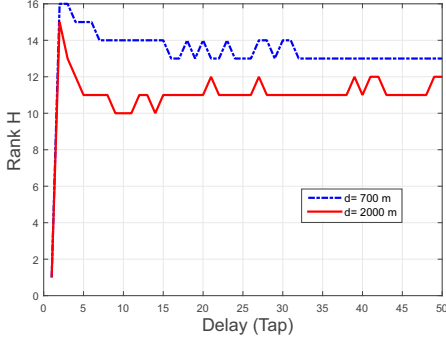
Fig. 7: Increasing the distance, the rank decreases due the presence of stronger LOS component

Fig. 8: BER in SISO en-route channel

based on the assumption that most of the energy of the channel is concentrated in the first tap $\mathbf{H}[k, \tau_1]$ (corresponding to the LOS) as observed in Figure 5.

Assuming full information of the channel $\mathbf{H}[k, \tau_1]$ at the transmitter, it is possible to perform *maximal eigen-beamforming* transmission by setting $N_s = 1$, which allocates only the strongest eigen-channel. Let $\hat{\mathbf{V}}$ and $\hat{\mathbf{U}}^H$ be the right and left singular vectors of $\mathbf{H}[k, \tau_1]$ corresponding to the strongest singular value σ_1 respectively. The channel symbols are first precoded using $\hat{\mathbf{V}}$ and then transmitted over the $N_{\text{Rx}} \times N_{\text{Tx}} \times L$ airborne channel $\mathbf{H}$, resulting in

$$\mathbf{y}[k] = \frac{1}{\sqrt{N_{\text{Tx}}}} \sum_{\tau_i=1}^{L} \mathbf{H}[k, \tau_i]\hat{\mathbf{V}}[k, \tau_1]\tilde{x}[k - \tau_i] + \mathbf{n}[k]. \quad (14)$$

The receiver finally applies $\hat{\mathbf{U}}^H$, resulting in

$$\tilde{y}[k] = \frac{1}{\sqrt{N_{\text{Tx}}}} \sum_{\tau_i=1}^{L} \hat{\mathbf{U}}^H[k, \tau_1]\mathbf{H}[k, \tau_i]\hat{\mathbf{V}}[k, \tau_1]\tilde{x}[k - \tau_i] + n[k]. \tag{15}$$

Assuming only knowledge of the direction of the receiver with respect to the transmitter, a linear detector has been implemented. The system implemented uses a linear MMSE filter able to suppress noise and inter-stream interference while the effect of the inter-symbol interference is still present. We design our MMSE receiver again based on the LOS component $\mathbf{H}[k, \tau_1]$:

$$\mathbf{U}_{\text{MMSE}}[k] = \left(\mathbf{H}^H[k, \tau_1]\mathbf{H}[k, \tau_1] + \frac{\sigma_n^2}{\sigma_s^2}\mathbf{I}_{N_{\text{Rx}}} \right)^{-1} \mathbf{H}^H[k, \tau_1]. \tag{16}$$

The filter linearly combines the received signal to form an estimation of the transmitted symbols

$$\tilde{\mathbf{y}}[k] = \mathbf{U}_{\text{MMSE}}^H[k]\mathbf{y}[k]. \tag{17}$$

To retreive the symbol $\tilde{y}[k]$ the received vector $\tilde{\mathbf{y}}[k]$ can now be coherently summed up.

C. System Simulation

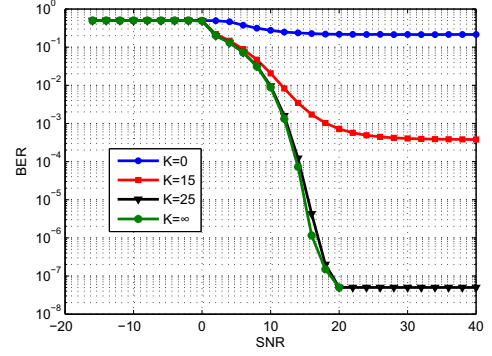The performance analysis is proposed for SISO and MIMO system. The BER performance was determined using a Monte Carlo simulation. Each simulation was conducted over 640 frames of data and averaged over 15 independents runs. The frames were interleaved with a length of 8 frames and have been split over each coherence time. The frequency used in the simulator was 5 GHz and the bandwidth was set to 10 MHz. Table I lists the parameters of the simulated channel for both the scenarios.

TABLE I: Simulation parameters

	En route scenario	Arrival scenario
v [m/s]	12	24
K factor [dB]	0, 15, 25, $+\infty$	0, 15, 25, $+\infty$
Slope PDP	-	$1\mu s$
d [m]	20000	2000
L	2	50
N	20	20

Figure 8 shows the performance for the two spike channel model in the en-route scenario, while Figure 9 shows the performance of the exponential PDP in the arrival scenario. The channel influences the BER introducing noise and time dispersion. By increasing the transmit power, the effect of the noise vanishes. The time dispersion, instead, leads to inter-symbol interference. The BER floor caused by the delay spread decreases for higher K, since the channel introduces less dispersion. The arrival scenario outperforms the en-route scenario because of the lower delay spread. While the two spike model presents a strong component with high delay, in the exponential distribution the channel spread is wider but in a shorter time lapse.

In multi-antenna system the performance is determined by the spread of the signal in space, in addition to the noise and the delay spread seen in the SISO case. The channel scenario presents a very strong LOS component, i.e., the matrix $\mathbf{H}$ has a low rank for low delays. The performance is strongly influenced by the LOS tap of the model, and both the transmission schemes yield to the same performances. In strong LOS, the full information of the channel at the transmitter does not conduce to further improvement with respect the classical beam shaping toward the receiver. All the possible 256 channels tend to have the same behavior because they follow the same physical path and change the direction of the beam by changing the coefficient $G_j^{\text{Tx}}(\hat{\mathbf{\Omega}}^{\text{Tx}})$ is equivalent
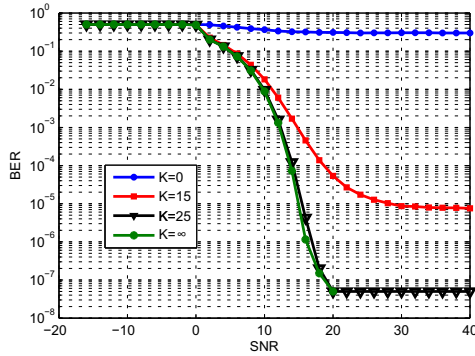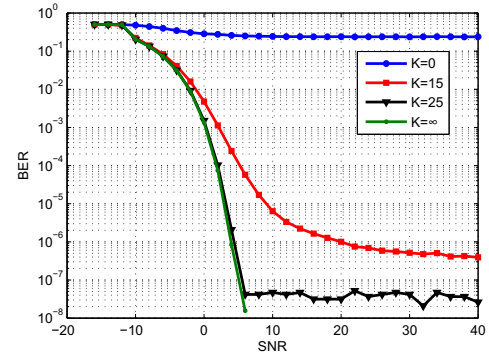
Fig. 9: BER in SISO arrival/takeoff channel
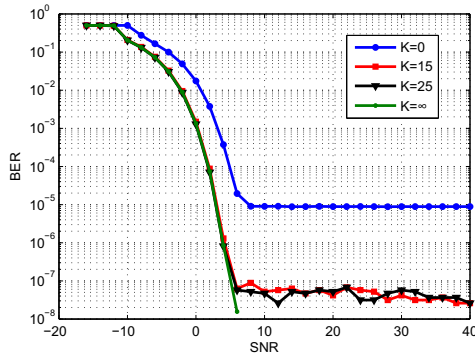

Fig. 11: BER in MIMO arrival/takeoff channel

Fig. 10: BER in MIMO en-route channel

scatterers spread the signal in the angular domain and worst performance are obtained in the arrival channel in which the presence of the scatters at very low distance heavily influences the final performance.

The extension of the model for a multi-antenna system has been interfaced with two transmission schemes, using different amount of channel state information at the transmitter, which equally perform due to the strong LOS application. The predicted enhancement, due to the use of the multi-antenna system, has been observed. Although the channel model developed has been based on assumption and measurement would need it, the coherence of the results with the theoretic expectation encourages the model to be proposed as a valid benchmark for an air-to-ground communication system.

to allocate the best eigen-channel. Therefore, the following the plots are valid for both transmission schemes.

The very long distance in the en route scenario creates the best condition to use a 16×16 MIMO as in Figure 10. Even for $K=0$, the BER is very close to the AWGN performance. For SNR greater than zero the performance is limited by the effects of the inter-symbol interference. Increasing the K the contribution of the interference tends to disappear. For $K = \infty$ the performance tends to the limit case of the AWGN channel obtaining the theoretical gain of 12 dB with respect the SISO case. Figure 11 shows the performance of the arrival channel. The BER floor remains and the proximity of the scatterers spreads the signal not only in time but also in space causing worst performances with respect the en route channel.

V. CONCLUSION

In this paper, the aeronautical channel was modeled and extended to the multi-antenna system including the spatial description. Simulations based on a single carrier wireless system have been conducted. In SISO system, the delay spread of the channel introduces an irreducible BER floor which is strongly depended on the power of the LOS. Moreover, different behavior has been observed for the en route and the arrival channel. The long distance and the altitude of the aircraft in the en route channel raises in higher delay spread and higher bit error probability.

The performance of the MIMO system are also influenced by the geometry of the environment. The presence of the

REFERENCES

[1] R. J., A. Aguasca, J. Alonso, S. Blanch, and R. Martins, "Small uav radiocommunication channel characterization," in *Antennas and Propagation (EuCAP), 2010 Proceedings of the Fourth European Conference on*, 2010.

[2] S. Elnoubi, "A simplified stochastic model for the aeronautical mobile radio channel," in *Vehicular Technology Conference, 1992, IEEE 42nd*, May 1992, pp. 960–963 vol.2.

[3] E. Haas, "Aeronautical channel modeling," *Vehicular Technology, IEEE Transactions on*, vol. 51, no. 2, pp. 254–264, 2002.

[4] W. Newhall and J. Reed, "A geometric air-to-ground radio channel model," in *MILCOM 2002. Proceedings*, vol. 1. IEEE, 2002, pp. 632–636.

[5] M. Steinbauer, A. F. Molisch, and E. Bonek, "The double-directional radio channel," *Antennas and Propagation Magazine, IEEE*, vol. 43, no. 4, pp. 51–63, 2001.

[6] S. M. Elnoubi, "A simplified stochastic model for the aeronautical mobile radio channel," in *Vehicular Technology Conference, 1992, IEEE 42nd*, 1992, pp. 960–963.

[7] P. Hoeher, "A statistical discrete-time model for the WSSUS multipath channel," *Vehicular Technology, IEEE Transactions on*, vol. 41, no. 4, pp. 461–468, Nov 1992.

[8] J. C. Liberti and T. S. Rappaport, "A geometrically based model for line-of-sight multipath radio channels," in *Vehicular Technology Conference, 1996. Mobile Technology for the Human Race., IEEE 46th*, vol. 2, 1996, pp. 844–848.

[9] "Acceptance-rejection method," in *Encyclopedia of Operations Research and Management Science*, S. Gass and M. Fu, Eds. Springer US, 2013, pp. 1–1. [Online]. Available: http://dx.doi.org/10.1007/978-1-4419-1153-7_200003

[10] M. Herdin, "Non-stationary indoor MIMO radio channels," Ph.D. dissertation, Institut für Nachrichtentechnik und Hochfrequenztechnik, Technische Universitat Wien.